

RSFQ devices with selective dissipation for quantum information processing

J. Hassel, H. Seppä and P. Helistö,
VTT Information Technology, Microsensing, P.O. Box 1207, 02044 VTT, Finland

We study the possibility to use frequency dependent damping in RSFQ circuits as means to reduce dissipation and consequent decoherence in RSFQ/qubit circuits. We show that stable RSFQ operation can be achieved by shunting the Josephson junctions with an RC circuit instead of a plain resistor. We derive criteria for the stability of such an arrangement, and discuss the effect on decoherence and the optimisation issues. We also design a simple flux generator aimed at manipulating flux qubits.

Rapid single flux quantum (RSFQ) technology [1] has been suggested as the classical interface for the quantum bits [2], and eventually for a scalable quantum computer. RSFQ technology is inherently dissipative. The dissipation is a likely source of decoherence, which limits the allowed coupling between the RSFQ circuit and the quantum circuit. It is caused by the damping of the Josephson junctions by shunt resistors. The conventional damping is, however, higher than what is needed for stable operation. Therefore one is encouraged to search solutions to decrease it. One approach is to use nonlinear damping in order to switch the damping on only, as a junction is switching [3]. Our approach, on the other hand, is based on the fact that the switching events occur at the time scale of the inverse plasma frequency. Therefore the damping at lower frequencies is redundant. The simplest way to realise the high-pass filtering is to connect a capacitor in series with the shunt resistor. One benefit is that such a circuit is realisable by a conventional Nb/AlOx trilayer process [4]. A similar approach has previously been suggested and tested to produce low-noise SQUID magnetometers [5, 6], and as means to improve the resolution of flux qubit readout circuits [7]. We now show that it is also possible to realise generic full-scale RSFQ circuits with such a configuration. As an example, we introduce a device design able to drive a qubit into a coherent superposition of flux states. The effect on the decoherence is also discussed.

In simple terms, the stability of an RSFQ circuit is guaranteed by the sufficient damping of the plasma resonances of the junctions and of the LC resonances formed by inductors and junction capacitances. The maximum (zero bias) angular plasma frequency is $\omega_p = 1/\sqrt{L_J C}$, where $L_J = \Phi_0/2\pi I_c$ is the Josephson inductance, C the capacitance and I_c the critical current of junction, and $\Phi_0 = h/2e$ is the flux quantum. Therefore the Q-value of the plasma resonance is chosen below unity. For a conventional damping scheme (see Fig. 1(a) and (b)), the square of the Q-value is given by the Stewart-McCumber parameter $\beta_c = 2\pi I_c R_s^2 C / \Phi_0$, where R_s is the shunt resistance and $\Phi_0 = h/2e$ is the flux quantum. The inductances of the RSFQ circuit elements are of the same order as the Josephson inductance (or $\beta_L \equiv 2\pi L I_c / \Phi_0 \sim 1$), so this simultaneously ensures the damping of the LC

resonances.

The junction parameters, inductances, and the shunt resistance can be similarly defined and their parameters chosen for the RC shunted RSFQ (Fig. 1(c)) as well. The additional component value to be chosen is the shunt capacitance C_s . From the discussion above it follows that a natural additional stability parameter is the ratio of the $R_s C_s$ cutoff and the plasma frequency, namely $\gamma = 1/\omega_p R_s C_s$. To test the effect of γ on the stability, we simulate the most basic RSFQ element, the Josephson transmission line (JTL). The value of $\beta_c = 1/2$ is fixed, while the bias point I_b and the capacitance C_s (or γ) are varied in order to test the stable range of parameters. We define the system to be stable, if the flux quantum propagates from the left end to the right end correctly as shown in Fig. 2(b). The indications of the lost stability are error pulses (in practice, the flux quantum reflecting back

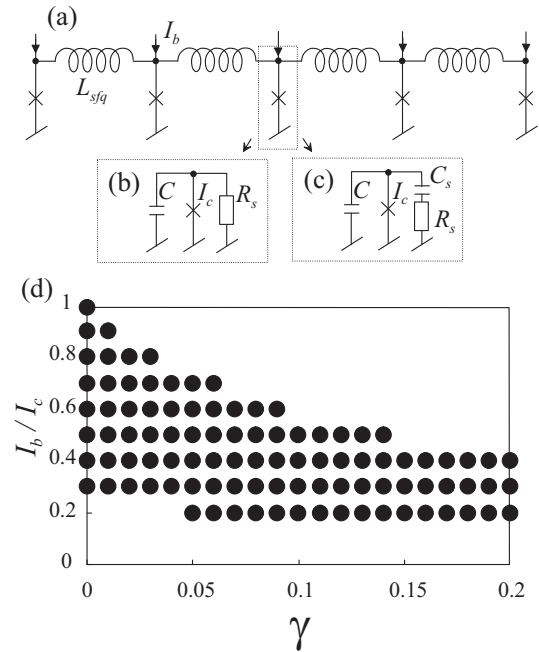


FIG. 1: (a) A Josephson transmission line realised with (b) conventional and (c) frequency dependent damping. (d) Stable parameter range as function of $\gamma = 1/R_s C_s \omega_p$ and the bias current I_b scaled to critical current I_c .

from the right end) or junctions switching permanently into a finite voltage state. The resulting stable parameter range is shown in Fig. 1(d). The leftmost column shows the corresponding result with the conventional JTL (formally with $C_s = \infty$). The decreased stability with RC damping and large bias currents is mainly because the potential barrier protecting against the error pulses is reduced. However, with realistic values of C_s sufficient stability can be obtained.

In a practical realisation of the shunt capacitance it is important to avoid parasitic resonances. The wavelength at the plasma frequency in the capacitor is given as $\lambda_p = 2\pi c / \omega_p \sqrt{\varepsilon_r (1 + 2\lambda_L/d)}$, where c is the speed of light, ε_r is the dielectric constant, λ_L is the London penetration depth of the electrodes, and d is the insulator thickness. To be on the safe side, the dimension of the capacitor should be $\lambda_p/8$ at maximum. Therefore for the capacitance (of a square) it applies $C_s \lesssim (\pi c)^2 \varepsilon_0 / 16 \omega_p^2 d (1 + 2\lambda_L/d)$. In other words, realizability dictates that

$$\gamma \gtrsim \frac{16\omega_p d (1 + 2\lambda_L/d)}{\pi^2 R_s c^2 \varepsilon_0} = \frac{32\sqrt{2}d (1 + 2\lambda_L/d)}{\pi \Phi_0 \varepsilon_0 c^2} I_c, \quad (1)$$

where in the last form the definition of the plasma frequency and $\beta_c = 1/2$ have been used. The minimum realizable γ depends only on the critical current, capacitor thickness and the London penetration depth. It is also favorable to use a small critical current, which is in accordance to minimising the heating effects. For example, an existing Nb process for milli-Kelvin applications has Nb₂O₅ capacitors with $d = 140$ nm, $\lambda_L = 90$ nm, and typically $I_c = 3$ μ A, whence it follows $\gamma \gtrsim 0.008$ thus enabling the operation well in the stable regime (see Fig. 1(d)).

We test next RC damping by simulating a simple device (Fig. 2(a)) able to generate rectangular fast rise-time flux-pulses. The device consists of two DC/SFQ converters [8] driving an RS flip-flop [1]. The generator takes two periodic (e.g. sinusoidal) mutually phase-locked signals as inputs, and produces a flux through the output coil L_{10} . The frequency of the flux pulses is the frequency of the input signals, and the pulse length is related to the phase difference of them. Resulting simulated time domain plots are shown in Figs. 2(b) and 2(c). The pulses with amplitude $\sim \Phi_0$ can e.g. be used in manipulating a flux-type qubit [9], provided the coupling between the device and the qubit is strong enough. With such a device one avoids the need of wide-band wiring and consequent noise from the room temperature electronics. A further benefit is relative simplicity.

The effect of drive and readout circuits on quantum circuits depends largely on the qubit type and the realisation of the classical circuit. Here we consider in general terms qubits, whose flux degree of freedom [10, 11, 12, 13, 14] is inductively coupled to an RSFQ

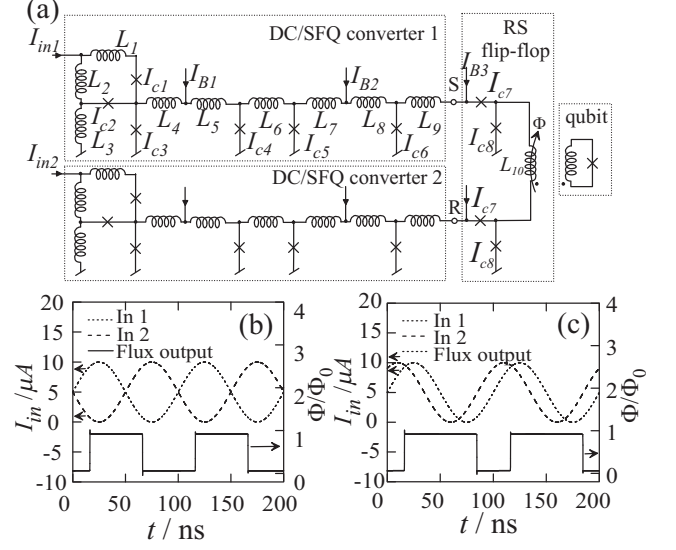


FIG. 2: (a) A flux pulse generator circuit coupled to a flux qubit. All the Josephson junctions of the RSFQ circuit are damped with RC shunts, which are not shown for clarity. (b) and (c) simulated time-domain plots of the RSFQ circuit. The parameters used here are $I_{c1} \dots I_{c7} = I_0$, $I_{c8} = 1.4I_0$, $I_{B1} = 1.6I_0$, $I_{B2} = 1.5I_0$, $I_{B3} = 0.7I_0$, where $I_0 = 2.9$ μ A and $L_1 = 0.35L_0$, $L_2 = 0.33L_0$, $L_3 = L_6 = 0.6L_0$, $L_4 = 0.1L_0$, $L_5 = 0.3L_0$, $L_7 = L_8 = 0.5L_0$, $L_9 = L_0$, and $L_{10} = 2.5L_0$, where $L_0 = 357$ pH. In addition $\omega_p = 2\pi \times 19$ GHz, $\beta_c = 0.5$ and $\gamma = 0.1$.

circuit (Fig. 3(a)). This type of an experiment benefits probably most from the frequency dependent damping.

The dissipation can be modelled as a frequency dependent effective resistance in parallel to the qubit inductance coupled to the RSFQ circuit (Fig. 3 (b)). The effective resistance R_{eff} is calculated for both conventional and RC shunted RSFQ in Fig. 3(c). For the conventional RSFQ R_{eff} is constant at low frequencies leading to constant dissipation

$$R_{eff,0} = b \frac{R_s}{k^2} \frac{L_q}{L_{sfq}}, \quad (2)$$

where L_q is an inductance of the qubit, L_{sfq} is the inductance of the RSFQ circuit, k is the coupling between the two, and b depends on the details of the RSFQ circuit. Taking only the nearest elements of the RSFQ circuit into account, we get $b = (1/2)(1 + 4(L_J L_{sfq} + L_{sfq}^2)/L_J^2)$, where the terms of order k^2 have been dropped. For the conventional RSFQ technology, the dissipation is ohmic, i.e. the environment spectral density $J_1(\omega) = (\pi/2) \alpha \hbar \omega$ [14, 15]. The decoherence time is typically inversely proportional to $J_1(\omega_q)$, where $\omega_q = \Delta E / \hbar$ with ΔE the energy level splitting of the qubit [15]. For a flux type qubit the dissipation parameter $\alpha = B \times R_q / R_{eff,0}$, where $R_q = h/4e^2$ is the quantum resistance and $B \sim 1$ is a constant dependent on the qubit details [9]. The minimum requirement for coherent operation (the weak-

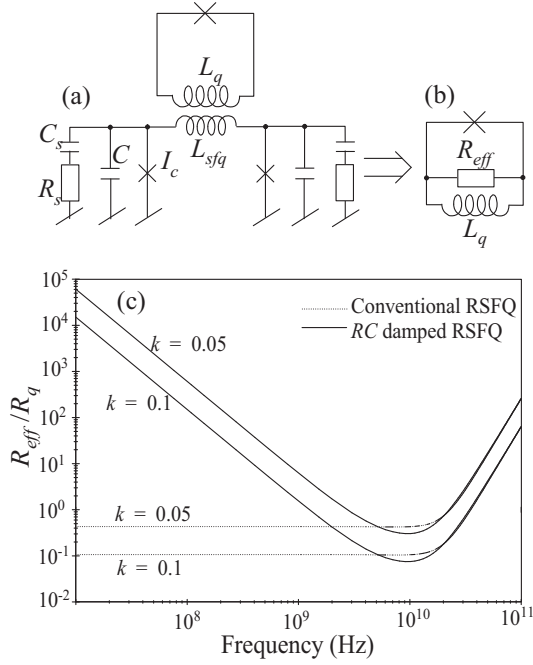


FIG. 3: Calculation of the effective damping resistance of a flux qubit coupled to an RSFQ circuit. The example parameters used here are $L_{sfq} = 357$ pH, $L_q = 10$ pH, $I_c = 3$ μ A, $\beta_c = 0.5$, and $\gamma = 0.2$.

damping limit) is that $\alpha \ll 1$. E.g. with parameters used in Fig. 3 this leads to the requirement of the coupling factor $k \ll 0.03$. This in turn leads to severe limitations in the resolution of a readout application, or a limited flux amplitude in the generation of drive signals.

In case of RC shunted RSFQ the corresponding figure is

$$R_{eff}(\omega) = \frac{R_{eff,0}}{(\omega R_s C_s)^2} = R_{eff,0} \left(\frac{\gamma \omega_p}{\omega} \right)^2. \quad (3)$$

This leads to superohmic spectral density $J_2(\omega) = (\pi/2) (\gamma \omega_p)^{-2} \alpha \hbar \omega^3$ [7, 15], and the improvement in the decoherence time (if limited by the RSFQ circuit) is $(\gamma \omega_p / \omega_q)^2$, provided $\omega_q \ll \gamma \omega_p$. This enables significant increase in k , even close to unity.

To optimise an RSFQ/qubit system, R_{eff} should be maximised. Since $R_{eff} \propto \gamma^2$ (Eq. (3)), γ should be chosen as large as possible. The drawback is, though, that the stability against the parameter spread is decreased (see Fig. 1(d)). Another possibility is to increase the plasma frequency, i.e. increase the critical current density J_c . It can be shown that R_{eff} is proportional to $J_c^{3/2}$, if L_q , the stability parameters and k are held constant. Therefore it is favorable to use large J_c , which is also favorable in terms on maximising the RSFQ speed. To simultaneously minimise the self-heating effects, one should have small I_c junctions [16]. Therefore large J_c

junctions with small areas are optimal. However, if the area is limited by the fabrication, one needs to compromise between the speed, the dissipation experienced by the qubit, and the heating effects.

The authors wish to thank M. Kiviranta, A. Kidiyarova-Shevchenko, J. Pekola, and A.O. Niskanen for useful discussions. The work was supported by EU through project RSFQubit (no. FP6-502807).

-
- [1] K. K. Likharev, and V. K. Semenov, IEEE Trans. Appl. Supercond. 1, 3, 1991.
 - [2] V. K. Semenov, D. V. Averin, IEEE Trans. Appl. Supercond. 13, 960, 2003.
 - [3] A. B. Zorin, M. I. Khabipov, D. V. Balashov, R. Dolata, F.-I. Buchholz, and J. Niemeyer, Appl. Phys. Lett. 86, 032501 (2005).
 - [4] L. Grönberg, J. Hassel, P. Helistö, M. Kiviranta, H. Seppä, M. Kulawski, T. Riekkinen, and M. Ylilammi, Extended abstracts of 10th International Superconductive Electronics Conference 2005, Noordwijkerhout, the Netherlands, 5-9 September 2005, O-W.04 (2005).
 - [5] H. Seppä, M. Kiviranta, V. Virkki, L. Grönberg, J. Salonen, P. Majander, I. Suni, J. Lnuutila, J. Simola, A. Oitinen, Extended Abstracts of 6th International Superconductive Electronics Conference, Braunschweig, Germany, 20 June 1997 (1997).
 - [6] M. Kiviranta, H. Seppä, Applied Superconductivity 6, 373 (1998).
 - [7] T. L. Robertson, B. L. T. Plourde, T. Hime, S. Linzen, P. A. Reichardt, F. K. Wilhelm, and J. Clarke, Phys. Rev. B 72, 024513 (2005).
 - [8] S. V. Polonsky, V. K. Semenov, P.I. Bunyk, A. F. Kirichenko, A. Yu Kidiyarova-Shevchenko, O. A. Mukhanov, P. N. Shevchenko, D. F. Schneider, D. Yu. Zinoviev, K. K. Likharev, IEEE Trans. Appl. Supercond. 3, 2566 (1993).
 - [9] Yu. Makhlin, G. Schön, A. Shnirman, Rev. Mod. Phys. 73, 357 (2001).
 - [10] J. E. Mooij, T. P. Orlando, L. Levitov, L. Tian, C. H. van der Wal, S. Lloyd, Science 285, 1036 (1999).
 - [11] I. Chiorescu, Y. Nakamura, C. J. P. M. Harmans, J. E. Mooij, Science 299, 1869 (2003).
 - [12] D. Vion, A. Aassime, A. Cottet, P. Joyez, H. Pothier, C. Urbina, D. Esteve, M. H. Devoret, Science 296, 886 (2002).
 - [13] B. L. T. Plourde, T. L. Robertson, P. A. Reichardt, T. Hime, S. Linzen, C.E. Wu, and J. Clarke, Phys. Rev. B 72, 060506 (2005).
 - [14] A. O. Caldeira, and A. J. Leggett, Phys. Rev. Lett. 46, 211 (1981).
 - [15] A. J. Leggett, S. Chakravarty, A. T. Dorsey, M. P. A. Fisher, A. Garg, W. Zwerger, Rev. Mod. Phys. 59, 1 (1987).
 - [16] A. M. Savin, J. P. Pekola, D. V. Averin, and V.K. Semenov, cond-mat/0509318